Mon. Not. R. Astron. Soc. **000**, 000–000 (0000) Printed 27 November 2009 (MN LaTeX style file v2.2)

New Wolf-Rayet star and its circumstellar nebula in Aquila⋆

V. V. Gvaramadze[1]†, A. Y. Kniazev[2,3], W.-R. Hamann[4], L. N. Berdnikov[1], S. Fabrika[5], and A. F. Valeev[5]

[1] *Sternberg Astronomical Institute, Moscow State University, Universitetskij Pr. 13, Moscow 119992, Russia*
[2] *South African Astronomical Observatory, PO Box 9, 7935 Observatory, Cape Town, South Africa*
[3] *Southern African Large Telescope Foundation, PO Box 9, 7935 Observatory, Cape Town, South Africa*
[4] *Institute for Physics and Astronomy, University Potsdam, 14476 Potsdam, Germany*
[5] *Special Astrophysical Observatory, Nizhnij Arkhyz, 369167, Russia*

Accepted 2009 November 26. Received 2009 November 26; in original form 2009 November 1

ABSTRACT

We report the discovery of a new Wolf-Rayet star in Aquila via detection of its circumstellar nebula (reminiscent of ring nebulae associated with late WN stars) using the *Spitzer Space Telescope* archival data. Our spectroscopic follow-up of the central point source associated with the nebula showed that it is a WN7h star (we named it WR 121b). We analyzed the spectrum of WR 121b by using the Potsdam Wolf-Rayet (PoWR) model atmospheres, obtaining a stellar temperature of $\simeq 50$ kK. The stellar wind composition is dominated by helium with ~ 20 per cent of hydrogen. The stellar spectrum is highly reddened ($E_{B-V} = 2.85$ mag). Adopting an absolute magnitude of $M_v = -5.7$, the star has a luminosity of $\log L/L_\odot = 5.75$ and a mass-loss rate of $10^{-4.7}$ $M_\odot$ yr^{-1}, and resides at a distance of 6.3 kpc. We searched for a possible parent cluster of WR 121b and found that this star is located at $\simeq 1$ degree from the young star cluster embedded in the giant H II region W43 (containing a WN7+a/OB? star – WR 121a). We also discovered a bow shock around the O9.5III star ALS 9956, located at $\simeq 0.5$ degree from the cluster. We discuss the possibility that WR 121b and ALS 9956 are runaway stars ejected from the cluster in W43.

Key words: line: identification – circumstellar matter – stars: individual: ALS 9956 – stars: Wolf-Rayet – open clusters and associations: individual: [BDC99] W43 cluster

1 INTRODUCTION

Wolf-Rayet (WR) stars are evolved massive stars possessing a strong stellar wind. Interaction of the WR wind with the material lost during the preceding evolutionary phase results in the origin of a compact circumstellar nebula (e.g. Chevalier & Imamura 1983; Robberto et al. 1993; Brighenti & D'Ercole 1995). The majority of WR circumstellar nebulae is associated with late WN-type (WNL) stars (Gvaramadze et al. 2009 and references therein), i.e. with stars that only recently entered the WR phase (e.g. Moffat, Drissen & Robert 1989). These nebulae could be sources of mid- and far-infrared (IR) emission (e.g. Mathis et al. 1992; Hutsemekers 1997; Marston et al. 1999) and can be detected with the modern IR surveys. Barniske et al. (2008) found circumstellar emission from dust and gas around two extremely luminous WN stars near the Galactic center.

The detection of compact nebulae reminiscent of nebulae associated with known WNL and Luminous Blue Variable (LBV) stars might suggest that their central stars are evolved massive stars as well and could be used for selection of candidate WNL, LBV or related stars for spectroscopic follow-ups. The importance of this channel for search for evolved massive stars was pointed out by Gvaramadze et al. (2009), who reported the discovery of a ring nebula in Cygnus (using the archival data from the Cygnus-X Spitzer Legacy Survey; Hora et al. 2009) and the results of spectroscopic follow-up of its central star, showing that the star belongs to the WN8-9h subtype. Inspired by this discovery, we searched for more ring nebulae in the archival data of the

⋆ Based on observations collected at the German-Spanish Astronomical Center, Calar Alto, jointly operated by the Max-Planck-Institut für Astronomie Heidelberg and the Instituto de Astrofísica de Andalucía (CSIC).

† E-mail: vgvaram@mx.iki.rssi.ru (VVG); akniazev@saao.ac.za (AYK); wrh@astro.physik.uni-potsdam.de (WRH); berdnik@sai.msu.ru (LNB); fabrika, azamat@sao.ru (SF, AFV)

© 0000 RAS

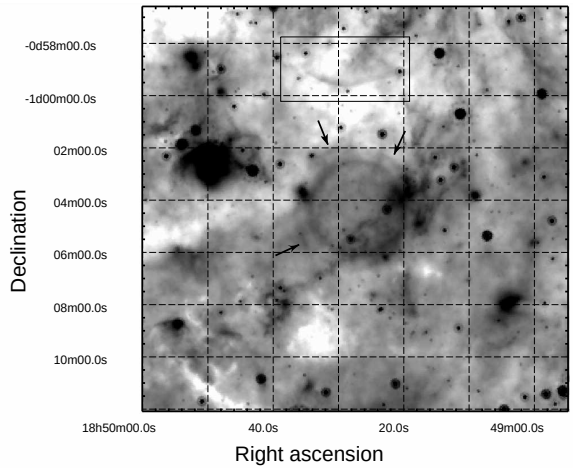

Figure 1. *Spitzer* MIPS 24 μm image of a new ring-like nebula in Aquila and its central star (WR 121b; located at the very centre of the ring). The signatures of a second incomplete concentric shell are indicated by three arrows. An arclike filament (surrounded by a rectangle) at $\simeq 3'$ to the north of the nebula is the south rim of the supernova remnant 3C 391.

Spitzer Space Telescope and found dozens of objects (Gvaramadze, Kniazev & Fabrika 2009; cf. Carey et al. 2009).

In this paper, we present the results of study of one of the stars selected via detection of their circumstellar nebulae. Our spectroscopic follow-up of this star showed that it is a WR star of the WN7h subtype, which provides a further proof of the effectiveness of our method for revealing massive post–main-sequence stars.

2 IR NEBULA AND ITS CENTRAL STAR

The new nebula in Aquila was discovered in the archival data of the *Spitzer Space Telescope*, obtained with the Multiband Imaging Photometer for *Spitzer* (MIPS; Rieke et al. 2004) within the framework of the 24 and 70 Micron Survey of the Inner Galactic Disk with MIPS (MIPSGAL; Carey et al. 2009). The MIPS 24 μm image of the nebula (see Fig. 1) shows a perfect circular shell with a diameter of $\simeq 3.8$ arcmin. One can see also signatures of a second incomplete concentric shell of diameter of $\simeq 4.6$ arcmin and some structures within the main shell; it is not clear, however, whether they are related to the nebula.

The region containing the nebula was also covered by the Galactic Legacy Infrared Mid-Plane Survey Extraordinaire (Benjamin et al. 2003) carried out with the Infrared Array Camera (IRAC; Fazio et al. 2004), the Multi-Array Galactic Plane Imaging Survey (Helfand et al. 2006), the SuperCOSMOS H-alpha Survey (SHS; Parker et al. 2005) and partially by *Chandra* observations of the (background) supernova remnant 3C 391 (located at $\simeq 3$ arcmin to the north of the IR shell). None of these observations nor the MIPS 70 μm data show signatures of the nebula.

Fig. 1 also shows a point source located exactly in the centre of the nebula, which suggests that this source might be associated with the nebula. The details of the source are summarized in Table 1. The coordinates and the J, H, K_s magnitudes are taken from the 2MASS All-Sky Catalog of Point Sources (Skrutskie et al. 2006).

Table 1. Details of the central star (WR 121b) associated with the new nebula in Aquila

RA(J2000)	$18^{\rm h}49^{\rm m}27\overset{\rm s}{.}34$
Dec.(J2000)	$-01^\circ04'20\overset{''}{.}8$
l, b	31.7515, -0.0480
V (mag)	17.15 ± 0.03
I (mag)	13.60 ± 0.03
J (mag)	10.94 ± 0.03
H (mag)	10.07 ± 0.03
K_s (mag)	9.47 ± 0.02
[3.6] (mJy)	77.8 ± 2.3
[4.5] (mJy)	70.6 ± 2.1
[5.8] (mJy)	55.5 ± 1.7
[8.0] (mJy)	37.6 ± 1.1
[24] (mJy)	9.7 ± 0.3
[70] (mJy)	< 3.1

The photometric V and I magnitudes of the optical counterpart to the IR central source were determined on a CCD frame obtained with the SBIG CCD ST-10XME attached to the 40-cm Meade telescope of the Cerro Armazones Astronomical Observatory of the Northern Catholic University (Antofagasta, Chile) during our observations in 2009 April. The accuracy of the measurements is $\simeq 0.03$ mag in both filters.

To measure the *Spizer*'s IRAC and MIPS fluxes from the star, we performed its aperture photometry using the `MOPEX/APEX` source extraction package and applied an aperture correction obtained from nearby bright point sources. The estimated errors are $\sim 2-3$ per cent. For the flux at 70 μm, we give a 3σ upper limit since the star was not detected at this wavelength.

3 SPECTROSCOPIC OBSERVATIONS AND DATA REDUCTION

To determine the nature of the central star associated with the new nebula in Aquila, we obtained its spectrum with the TWIN spectrograph attached to the Cassegrain focus of the 3.5 m telescope in the Observatory of Calar Alto (Spain) during director's discretionary time on 2009 May 5. The setup used for TWIN was the grating T08 in the first order for the blue arm (spectral range 3500–5600 Å) and T04 in the first order for the red arm (spectral range 5300–7600 Å) which provides with an inverse dispersion of 72 Å/mm for both arms. We have used the CCD detectors SITe#22b_14 and SITe#20b_12 for the blue and red arms, respectively, with the 5500 Å beam splitter. A slit of $240'' \times 2.1''$ was used for these spectral observations. The resulting FWHM spectral resolution measured on strong lines of the night sky and reference spectra was 3–3.5 Å. The seeing during the observations was stable, $\simeq 1.5-1.6$ arcsec. The observations were carried out at relatively low airmasses ($1.25-1.40$) and the slit was aligned exactly to the parallactic angle to exclude any atmospheric dispersion effects. The total exposure of 3600 s was broken up into three 1200 s subexposures to

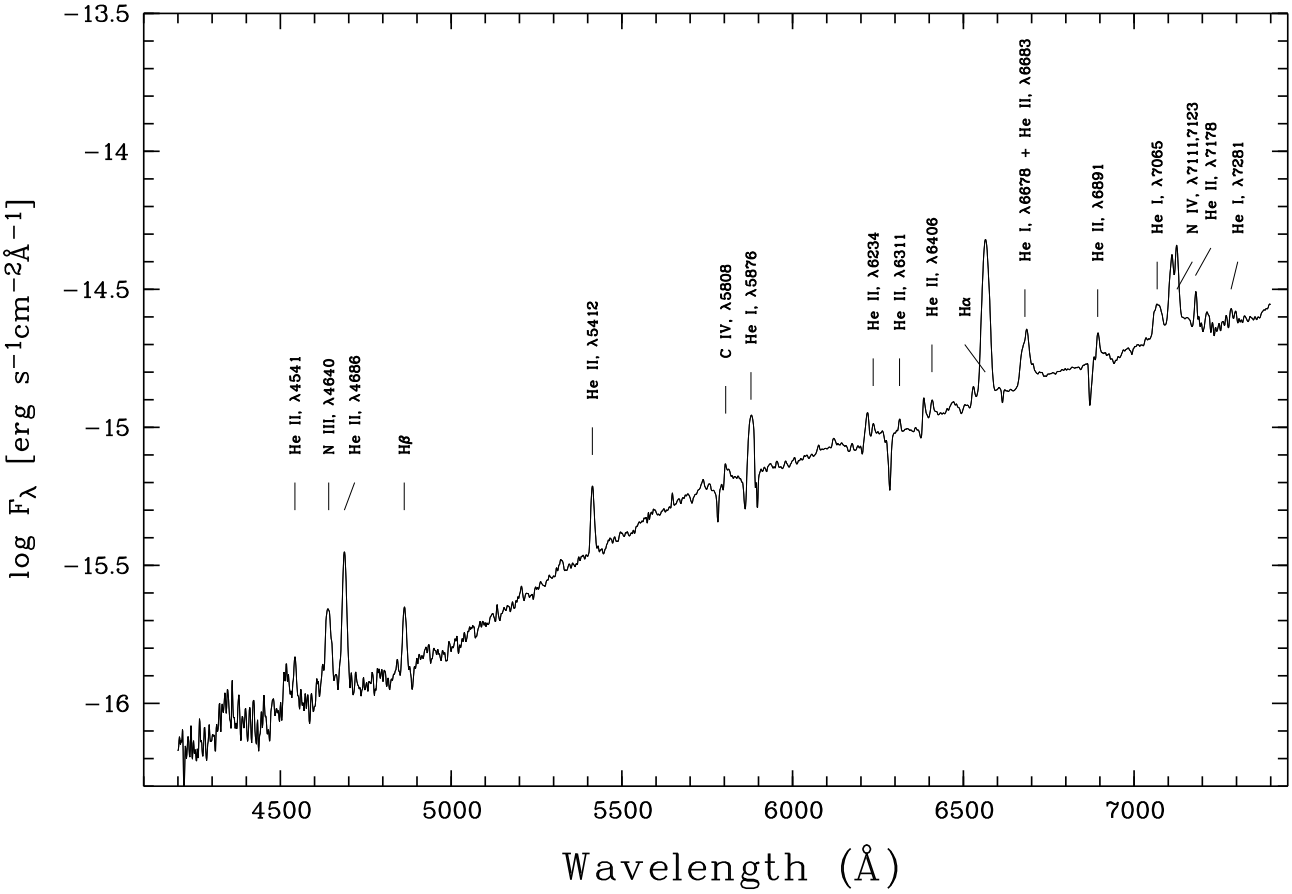

Figure 2. The observed spectrum of the central star (WR 121b) associated with the new nebula in Aquila with the most prominent lines indicated.

allow for removal of cosmic rays. Spectra of He–Ar comparison arcs were obtained to calibrate the wavelength scale. The spectrophotometric standard star BD+33° 2642 (Oke 1990; Bohlin 1996) was observed at the beginning for flux calibration.

The primary data reduction was done using the IRAF[1] package `ccdred`. The data for each CCD detector were trimmed, bias subtracted and flat corrected. We used the IRAF software tasks in the `twodspec` package to perform the wavelength calibration and to correct each frame for distortion and tilt. To derive the sensitivity curve, we fitted the observed spectral energy distribution of the standard star by a low-order polynomial. The final sensitivity curves have an internal precision better than 1 per cent over the whole optical range. One-dimensional (1D) spectra were then extracted using the IRAF APALL task. All one-dimensional spectra obtained with the same setup were then averaged. Finally, the blue and red parts of the total spectrum were combined without additional factors. The resulting reduced spectrum is shown in Fig. 2.

[1] IRAF: the Image Reduction and Analysis Facility is distributed by the National Optical Astronomy Observatory, which is operated by the Association of Universities for Research in Astronomy, In. (AURA) under cooperative agreement with the National Science Foundation (NSF).

The main emission lines were measured applying the MIDAS programs described in detail in Kniazev et al. (2004, 2008a). Their equivalent widths (EW), FWHM and heliocentric radial velocities are summarized in Table 2.

4 A NEW WOLF-RAYET STAR – WR 121B

4.1 Spectral type

Fig. 2 shows that the spectrum of the central star of the new nebula in Aquila is dominated by strong emission lines of hydrogen, He I, He II, N III and N IV. A less pronounced emission line of C IV is also present in the spectrum. Many of the weaker lines show P Cygni profiles, while the strongest lines are entirely in emission. Numerous absorptions visible in the spectrum are either interstellar [e.g. diffuse interstellar bands (DIBs) at $\lambda\lambda 4428, 4726, 4762, 5780, 5797$ and 6280] or (for $\lambda \gtrsim 7200$ Å) telluric in origin. No forbidden lines can be seen in the spectrum.

The prominent helium and nitrogen emission lines indicate that the star belongs to the nitrogen sequence of Wolf-Rayet stars (WN). To determine its WN subtype we apply the three-dimensional classification scheme by Smith et al. (1996). The measured line ratios He II λ5412/He I λ5876, C IV λ5808/He II λ5412 and C IV λ5808/He I λ5876 ($\simeq$ 0.9, 0.2 and 0.2, respectively) suggest that the star be-

Table 2. Equivalent widths (EW), FWHM and heliocentric radial velocities of main emission lines.

λ_0(Å) Ion	EW(λ) [Å]	FWHM(λ) [Å]	V_{hel} [km s^{-1}]
4541 He II	5.3±2.3	12.4±0.8	77±11
4640 N III	27.1±6.6	22.7±0.9	131±11
4686 He II	33.8±4.0	13.9±0.3	124±6
4861 He II+Hβ	10.2±2.8	12.3±0.6	143±8
5412 He II	8.9±1.0	10.7±0.2	142±5
5808 C IV	2.5±0.6	20.0±2.2	
5876 He I	11.2±1.0	14.0±1.0	164±10
6234 He II	0.9±0.2	7.9±0.4	148±6
6311 He II	0.4±0.1	4.2±1.3	132±11
6406 He II	1.6±0.3	10.0±0.6	130±8
6563 He II+Hα	63.2±0.7	21.3±0.1	133±4
6678 He I+He II	14.9±0.7	27.3±0.5	
6891 He II	2.9±0.5	10.6±1.8	186±12
7065 He I	11.5±0.8	29.8±2.0	
7111 N IV	14.2±0.5	14.4±0.9	140±9
7123 N IV	14.3±0.5	12.8±0.7	120±8
7178 He II	3.8±0.3	9.6±0.6	142±10
7281 He I	0.8±0.1	6.3±1.0	129±12

longs to the WN7 subtype. The same classification follows from the position of WR 121b in the plot of He II λ5412 EW versus He II λ4686 FWHM [see Fig. 13 and Fig. 15 of Smith et al. (1996) and Table 2].

The hydrogen Balmer lines coincide with the lines of the He II Pickering series $4-n$ for even principle quantum numbers n. The quantitative analysis (see below) will reveal that the He II blends with Hα and Hβ are stronger than predicted by a hydrogen-free model that fits the unblended He II 7-4 line at 5412 Å. Hence there is a detectable contribution from hydrogen to these line blends. This conclusion can be justified by using the empirical 'hydrogen criteria' for WN stars introduced by Smith et al. (1996). For EWs of lines at 4861, 4541 and 5412 Å given in Table 2, one finds a ratio $\mathrm{EW}(4861)/[\sqrt{\mathrm{EW}(4541)\mathrm{EW}(5412)}-1]=1.7$, which is much larger than 0.5, the figure defining the presence of hydrogen. Following the three-dimensional classification for WN stars by Smith et al. (1996), we therefore add a suffix 'h' to the spectral subtype, which then becomes WN7h.

We name our program star WR 121b, in accordance with the numbering system of the VIIth Catalogue of Galactic Wolf-Rayet Stars by van der Hucht (2001).

4.2 Nebular emission

The red part of 2D spectrum shows a complex of emission lines originating in the region covered by the slit. The intense emission lines include, in particular, Hα, [N II] λ6584, and [S II] $\lambda\lambda$6716, 6731. The ratios of the line fluxes (log([N II]/Hα)=−0.73, log([S II]/Hα)=−0.58, [S II](6717/6731)=1.3) clearly show that the lines originate in a hot tenuous medium, which is most likely an extended H II region [see, e.g., the diagnostics of H II regions by Kniazev et al. (2008b)]. The intensities of all these lines are very uniform along the slit. The Hα radial velocity [measured in the way described by Zasov et. al. (2000)] is also constant (36 ± 4 km s^{-1}) along the slit. We conclude therefore that the nebular line emission originates from an H II region unrelated to WR 121b and its ring nebula.

This conclusion is supported by an estimate of the interstellar extinction from the Balmer decrement. We found $A_V=4.6$ mag (constant along the slit), which is much less than $A_V=8.8$ mag derived from the stellar spectrum (see Section 4.4).

4.3 Spectral analysis and stellar parameters

To analyze the stellar spectrum and to derive the fundamental parameters of WR 121b, we use the Potsdam Wolf-Rayet (PoWR) models for expanding stellar atmospheres. These models acount for complex model atoms including iron-line blanketing in non-LTE (for a detailed description see Hamann & Gräfener 2004). For abundances of trace elements we adopt mass fractions which are typical for Galactic WN stars – N: 0.015, C: 0.0001, Fe: 0.0014 per cent (Hamann & Gräfener 2004).

The main parameters of a WR-type atmospheres are the stellar temperature, T_*, and the so-called transformed radius, $R_{\rm t}$. The stellar temperature T_* denotes the effective temperature related to the radius R_*, i.e. $L=\sigma T_*^4 4\pi R_*^2$, where σ is the Stefan-Boltzmann constant and R_* is by definition at a Rosseland optical depth of 20. $R_{\rm t}$ is related to the mass-loss rate $\dot{M}$ and defined by

$$R_{\rm t}=R_*\left[\frac{v_\infty}{2500\ {\rm km\,s^{-1}}}\Bigg/\frac{\sqrt{D}\dot{M}}{10^{-4}\ {\rm M_\odot\,yr^{-1}}}\right]^{2/3}, \qquad (1)$$

where D is the clumping contrast, and v_∞ is the terminal velocity of the wind.

These basic stellar parameters T_* and $R_{\rm t}$ are determined from fitting the lines in the normalized spectrum (see Fig. 3). The normalization is in fact achieved by dividing the absolutely calibrated observed spectrum by the theoretical continuum, which makes the total procedure described in the following an iterative process.

A first orientation about the proper choice of these parameters can be obtained by comparing the observed spectrum to the published grids of WN models (Hamann & Gräfener 2004). With respect to the stellar temperature, we select the model which reproduces best the balance between the lines from He I versus He II. At the same time, $R_{\rm t}$ is properly chosen which influences the strength of the emission lines in general. Conveniently, the grid model WNL07-11 [T_* = 50 kK, $\log(R_{\rm t}/R_\odot)=1.0$] provides a satisfactory fit to the observed line spectrum (see Fig. 3). Note that according to its location in the transformed radius-temperature diagram (Hamann & Gräfener 2004), WR 121b belongs to the WN7 subtype, consistent with our classification in Section 4.1.

The terminal wind velocity of $v_\infty=1000$ km s^{-1}, for which the grid had been calculated, nicely reproduces the widths of the line profiles and thus obviously adequate for our star.

The clumping contrast D [cf. equation (1)] has influence on the electron-scattering wings of strong emission lines. Hamann & Koesterke (1998) established $D=4$ as a typical value for WN stars. The model grid from Hamann & Gräfener (2004) which we use here is calculated with $D=4$, and therefore we keep this choice for practical reasons. Recent discussions (see Hamann et al. 2008) favour stronger

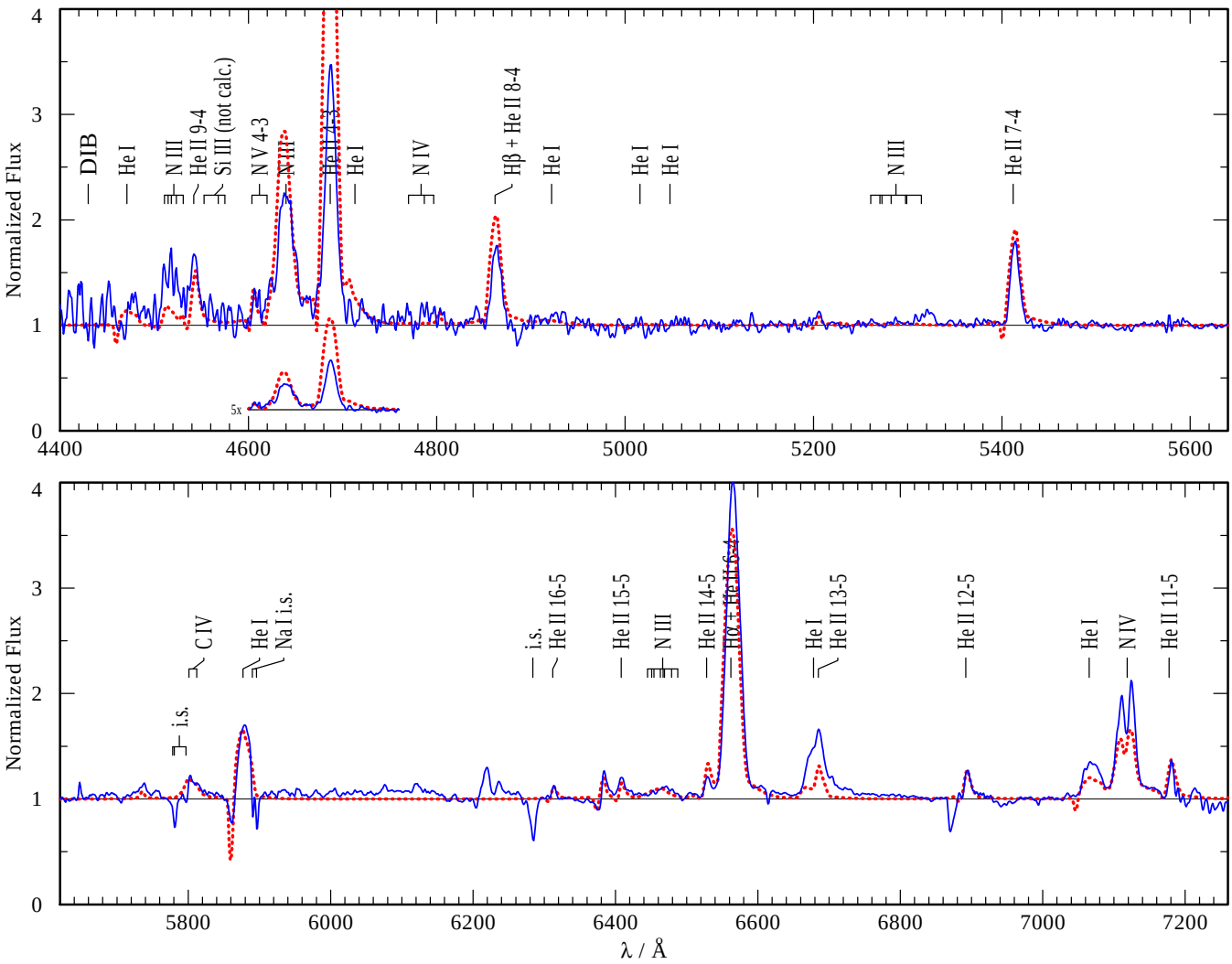

Figure 3. Observed optical spectrum (blue/solid line) of WR 121b, compared with the best-fitting model (red/dotted line) with the parameters as given in Table 3. For normalization the absolutely calibrated observation was divided by the reddened model continuum, and after slightly aligned further "by eye".

clumping up to $D = 10$. Data and fit quality do not allow an individual estimate of D for WR 121b to this precision, but values smaller than 4 can be ruled out e.g. from the red wing of Hα/He II 6-4. Note that the effect of D is simply a scaling of the empirically derived mass-loss rate proportional to $D^{-1/2}$.

The WNL model grid is calculated with a hydrogen abundance ($X_{\rm H}$) of 20 per cent by mass. For a closer check we compare the fit with models of zero hydrogen and with 40 per cent hydrogen. Fig. 4 shows the lines of the He II Pickering series (8–4: 4862 Å; 7–4: 5412 Å; 6–4: 6562 Å). Those profiles that are blended with Hβ (left frame) or Hα (right frame) become much stronger with growing hydrogen abundance, while the unblended He II line at 5412 Å (middle frame) becomes slightly weaker because of the compensating decrease of helium. The comparison with the observed profiles (blue/thick solid lines in Fig. 4) reveals that the hydrogen-free model predicts a too small line at the Hα wavelength, while with 40 per cent hydrogen Hα and Hβ are both stronger in the model than observed. Hence the hydrogen abundance of 20 per cent is a good estimate, and we can consider the grid model as our best fit.

4.4 Luminosity and distance of WR 121b

The spectral analysis alone cannot tell the absolute dimensions of the star. These are related to the distance of the object, which is a priori unknown for WR 121b.

However, a couple of Galactic WN stars can be assigned to open clusters or associations for which the distance can be independently determined. On this basis, correlations between the absolute magnitude and the spectral subtype have been established.

Hamann et al. (2006) have shown that stars with WN7 subtype come in two flavours. Some WN7 stars belong to the group of extremely bright and luminous WNL stars that come from very massive progenitors. Their absolute magnitude is about $M_v = -7.2$ mag (v magnitudes refer to the monochromatic flux at 5160 Å), and their winds typically

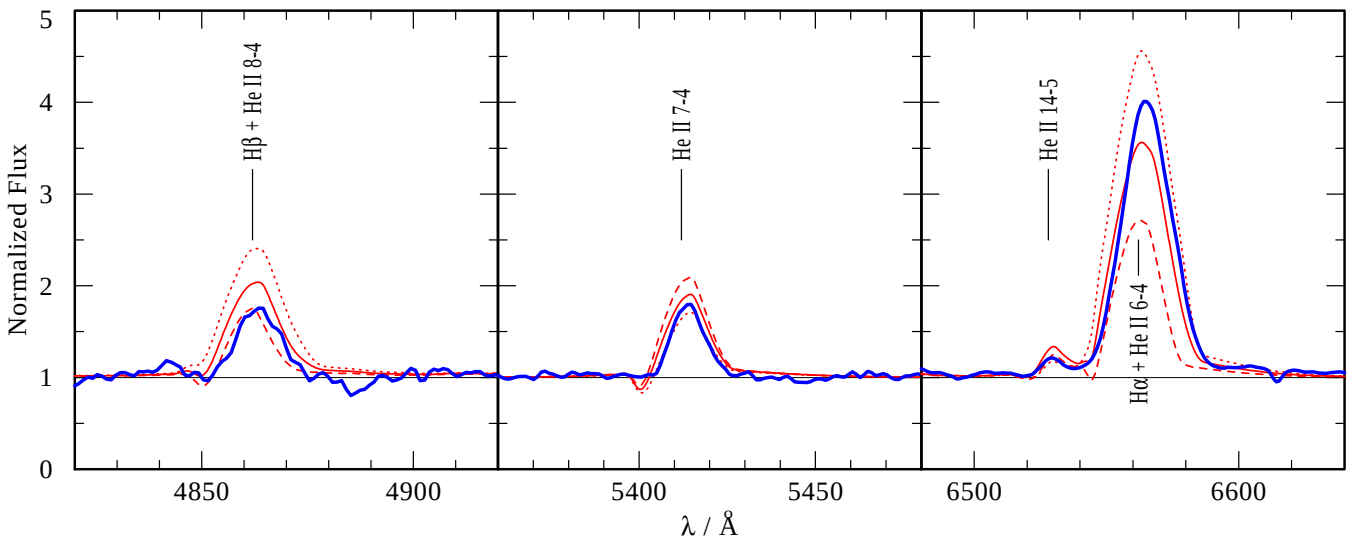

Figure 4. Test for the hydrogen abundance in WR 121b. The observed profiles (blue/thick solid line) are compared with models (red/thin lines) for different hydrogen abundance, but otherwise the same parameters as of our best-fit model (see Table 3). The tested hydrogen mass fractions are zero (dashed lines), 20 per cent (thin solid lines) and 40 per cent (dotted lines), respectively.

show a high hydrogen abundance of about 50 per cent by mass.

However, stars of the spectral subtype WN7 can also belong to an extension of the "early" subtypes (WNE), which are less luminous. According to the subtype calibration by Hamann et al. (2006), a WN7 star of this kind would have an absolute magnitude of $M_v = -5.7$ mag (with an uncertainty of about 0.5 mag). Most of the WNE stars are hydrogen-free, but some of them show a small hydrogen mass fraction below 25 per cent. According to the hydrogen content of about 20 per cent determined above, WR 121b rather belongs to this group of less bright stars.

Therefore we now scale our best-fit grid model to an absolute brightness of $M_v = -5.7$ mag. Remember that, in fair approximation, WR models of the same "transformed radius" $R_{\rm t}$ [see equation (1)] can be scaled to different absolute sizes. The scaled model has a luminosity of $\log L/L_\odot = 5.75$ (cf. Table 3). The corresponding stellar radius, mass-loss rate and the number of hydrogen-ionizing photons ($\Phi_{\rm i}$) are included in the same table. Note that the error estimates given in Table 3 are rough and based on the experience that the line fit is accurate to one cell of the model grid, i.e. to 0.05 in $\log T$ and to 0.1 in $\log R_{\rm t}$. The main uncertainty in the luminosity and the distance comes from the subtype calibration of the absolute visual magnitude. The given mass-loss rate refers to the adopted clumping parameter of $D = 4$. The uncertainty in the mass-loss rate is mainly due to the error margin of the luminosity, since the empirical $\dot{M}$ scales proportional to $L^{2/3}$.

The spectral energy distribution (SED) of the scaled model is now fitted to the photometric observations (Fig. 5). Two parameters can be adjusted for the fit, the distance d and the reddening E_{B-V}. The reddening law we adopt from Seaton (1979) in the optical and from Moneti et al. (2001) in the IR. A perfect fit to the whole SED is achieved with $E_{B-V} = 2.85$ mag and $d = 6.3$ kpc. The strong interstellar absorption also shows up in the observed spectrum by pronounced DIBs (see Fig. 2). The high reddening implies an extinction in the visual of $A_V = 8.8$ mag and a severe decrease of the flux at shorter wavelengths; for $\lambda < 4400$ Å our observed optical spectrum drowns in the noise.

Table 3. Stellar parameters for WR 121b

Spectral type	WN7h
T_* [kK]	50±5
$\log R_{\rm t}\,[R_\odot]$	10±4
$v_\infty\,[{\rm km\,s^{-1}}]$	1000±200
$X_{\rm H}$	0.2±0.1
$\log L\,[L_\odot]$	5.75±0.30
$R_*\,[R_\odot]$	10.0±2.0
$\log \dot{M}\,[{\rm M_\odot yr^{-1}}]$	-4.7±0.3
$\log \Phi_{\rm i}\,[{\rm s^{-1}}]$	49.6±0.3
E_{B-V} [mag]	2.85±0.05
d [kpc]	$6.3^{+2.2}_{-1.6}$

5 POSSIBLE BIRTH CLUSTER OF WR 121B

WR 121b, like the majority of WR stars, is located outside of known star clusters. Since most of massive stars originate in a clustered mode of star formation (e.g. Zinnecker & Yorke 2007), it is natural to assume that WR 121b (or its progenitor star) was ejected from the parent cluster either through a dynamical process in the core of the cluster (Poveda et al. 1967; Gies & Bolton 1986) or due to a supernova explosion in a close massive binary system (Blaauw 1961; Stone 1991). The first process could start to operate at the very beginning of cluster evolution, while the second one only several Myr after the cluster formation, when the most massive stars in binaries (and respectively in the cluster) end their lives as supernovae. In both cases, the ejected WR star should not be far from its parent cluster since the progenitors of WR

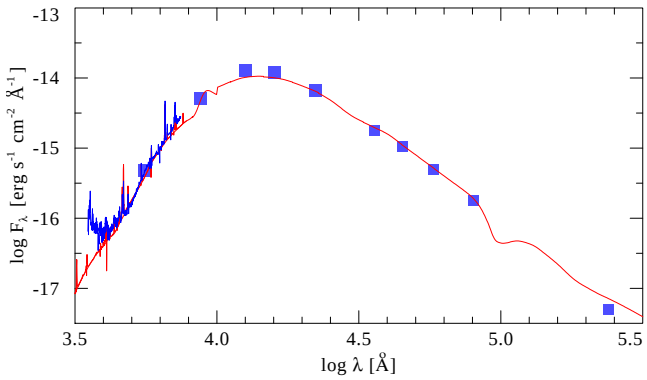

Figure 5. Observed flux distribution of WR 121b (blue/noisy) in absolute units, including the calibrated spectrum and the photometric measurements compiled in Table 1, compared to the emergent flux of the model continuum (red/smooth line), in the optical also shown with lines. The model flux has been reddened and scaled to the distance according to the parameters given in Table 3.

stars are very massive ($\gtrsim 25$ M$_\odot$) and therefore short-lived ($\lesssim 5$ Myr) stars.

Proceeding from the aforementioned, we searched for known young star clusters around WR 121b using the SIMBAD[2] and WEBDA[3] databases and found that this star is located at ~ 1 degree from a cluster deeply embedded ($A_V \simeq 30$ mag) in the giant H II region W43 (see Fig. 6). This cluster (named in the SIMBAD database as '[BDC99] W43 cluster') contains at least three evolved massive stars (Blum, Damineli & Conti 1999), two of which are O-type giants or supergiants and the third one is a WN7+a/OB? star (WR 121a).

The large ionizing flux of the W43 star forming region ($\sim 10^{51}$ Lyman continuum photons s^{-1}; Smith, Biermann & Mezger 1978) is comparable with that of the very massive star cluster NGC 3603, which suggests that the central cluster in W43 contains a large number of yet undetected massive stars and therefore should be effective in producing runaway stars (e.g. Gvaramadze 2009; Gvaramadze, Gualandris & Portegies Zwart 2008, 2009). On the other hand, the presence of the WNL star in the cluster implies that the age of the cluster is comparable to the evolutionary age of WR 121b. It is plausible, therefore, to identify the origin of WR 121b (or its progenitor star) with the central cluster of W43.

This conjecture is also supported from the distance to WR 121b of $6.3^{+2.2}_{-1.6}$ kpc which we have obtained in Section 4.4. For W43 a distance of about 7 kpc was derived from H I radio measurements and a Galactic rotation model (Wilson et al. 1970), which for the modern value of the distance to the Galactic Centre reduces to about 5.6 kpc (Blum et al. 1999). Blum et al. (1999) obtained 5.7 kpc from two O stars observed in W43 when assuming that they are giants. Thus, within the error margins the distances are consistent.

With a luminosity of $\log L/L_\odot \simeq 5.75$, the current and the initial masses of WR 121b are ~ 20 and 40 M$_\odot$, respectively, and its evolutionary age is $\simeq 4-5$ Myr. The latter

[2] http://simbad.u-strasbg.fr/simbad/
[3] http://www.univie.ac.at/webda/

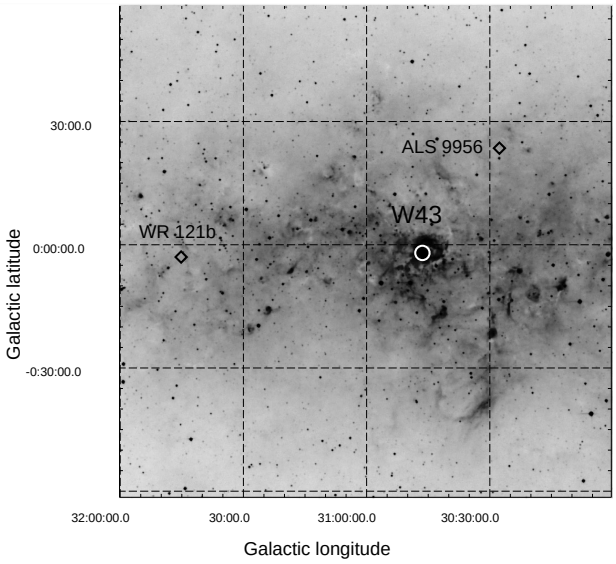

Figure 6. A $2^\circ \times 2^\circ$ 8.28 μm image of the H II region W43 and its environments obtained in the *Midcourse Space Experiment* Galactic plane survey (Price et al. 2001), with the position of the star cluster embedded in W43 marked by a white circle and the positions of WR 121b and ALS 9956 indicated by diamond points. See text for details.

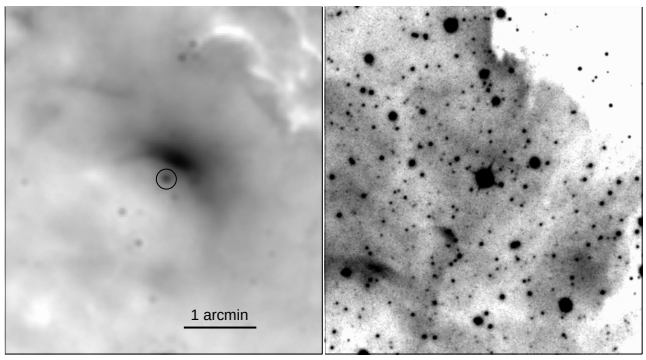

Figure 7. *Left*: *Spitzer* MIPS 24 μm image of ALS 9956 (marked by a circle) and its bow shock. *Right*: SHS image of the same field. Orientation of these images is the same as for Fig. 6.

estimate and the angular separation between WR 121b and W43 ($\simeq 1$ degree, which for $d = 6.3$ kpc corresponds to the linear separation of $\simeq 110$ pc) implies that the minimum allowed peculiar (transverse) velocity of WR 121b is ~ 25 km s^{-1}. We predict, therefore, the 'observed' (i.e. not corrected for the Galactic rotation and the solar motion) proper motion of WR 121b of $\mu_\alpha \simeq -1.6$ mas yr^{-1} and $\mu_\delta \simeq -3.7$ mas yr^{-1} (if the star was ejected $\simeq 4-5$ Myr ago) or $\mu_\alpha \simeq -0.3$ mas yr^{-1} and $\mu_\delta \simeq -1.2$ mas yr^{-1} (if the the ejection occurred ~ 1 Myr ago). [These estimates were derived using the Galactic constants $R_0 = 8$ kpc and $\Theta = 200$ km s^{-1} (e.g. Reid 1993; Avedisova 2005) and the solar peculiar motion $(U_\odot, V_\odot, W_\odot) = (10.00, 5.25, 7.17)$ km s^{-1} (Dehnen & Binney 1998).] Proper motion measurements for WR 121b are necessary to prove the association between this star and the star forming region W43 and thereby to constrain some of its inferred fundamental parameters.

To find the evidence that the [BDC99] W43 cluster loses its massive stars, we searched for bow shock-like structures in its environments using the MIPSGAL survey. The visual inspection of MIPS 24 μm images results in the discovery of a bow shock produced by the O9.5III star ALS 9956 (see Fig. 7), located at $\simeq 0.5$ degree from the cluster (see Fig. 6). The bow shock has an obvious optical counterpart in the SHS. The orientation of the symmetry axis of the bow shock and the evolutionary age of the star of $\sim 4-5$ Myr are consistent with a possibility that ALS 9956 was ejected from the cluster in W43 (cf. Gvaramadze & Bomans 2008).

Further support to this possibility comes from comparison of the (photometric) distance to ALS 9956 with the distance to the cluster. ALS 9956 has the B and V magnitudes of, respectively, 11.83 and 11.25 (Kharchenko 2001). Using the extinction law from Rieke & Lebofsky (1985) and the synthetic photometry of Galactic O stars by Martins & Plez (2006), we derived extinction towards ALS 9956 of $A_{\rm V} \simeq 2.6$ mag and estimated the distance to this star to be 6.2 kpc, i.e. similar to the distance to the cluster.

Using the VizieR catalogue access tool[4], we searched for proper motion measurements for ALS 9956 and found that all existing measurements are insignificant (i.e. the measurement uncertainties are comparable to the measurements themselves) and, therefore, cannot be used to prove unambiguously our hypothesis that the star was ejected from W43. Still, taken at face value, they suggest that ALS 9956 is a runaway star moving away from the Galactic plane towards growing Galactic latitude (which is consistent with the position of the star above the Galactic plane), while the direction of stellar motion inferred from the symmetry of the bow shock (see, e.g., Gvaramadze & Bomans 2008) is well within the stellar proper motion error cone.

We note that the visual extinction towards ALS 9956 and WR 121b is much smaller than that towards the [BDC99] W43 cluster. If both stars were indeed ejected from the cluster, then we conclude that some OB stars can be detected in optical wavelengths only because they are runaway stars, while their cousins residing in the parent clusters might still remain totally obscured. This may explain why some field O-type stars show no apparent association with star clusters [cf. de Wit et al. (2005); Schilbach & Röser (2008); Gvaramadze & Bomans (2008)].

6 CONCLUSION

We have discovered a new WNL (WN7h) star via detection of a circular IR nebula (typical of evolved massive stars) and spectroscopic follow-up of its central star. This discovery provides further evidence that the circumstellar nebulae associated with WR stars are inherent almost exclusively to WR stars of the WNL subclass. It also shows that the IR imaging could be an effective tool for revealing WNL and related evolved massive stars. The new WNL star is one of many dozens of (candidate) evolved massive stars revealed via their association with compact IR nebulae, detected in the MIPS 24 μm data from the *Spitzer Space Telescope* archive. The spectroscopic study of these stars is currently underway and its results will be presented in the forthcoming papers.

[4] http://webviz.u-strasbg.fr/viz-bin/VizieR

7 ACKNOWLEDGEMENTS

We thank the Calar Alto Observatory for allocation of director's discretionary time to this programme and A.F.J.Moffat (the referee) for suggestions and comments allowing us to improve the presentation of the paper. AYK acknowledges support from the National Research Foundation. SF and AFV acknowledge support from the RFBR grant N 09-02-00163. This work is based in part on archival data obtained with the Spitzer Space Telescope, which is operated by the Jet Propulsion Laboratory, California Institute of Technology under a contract with NASA, and has made use of the NASA/IPAC Infrared Science Archive, which is operated by the Jet Propulsion Laboratory, California Institute of Technology, under contract with the National Aeronautics and Space Administration. This research has made use of the SIMBAD database and the VizieR catalogue access tool, both operated at CDS, Strasbourg, France, and the WEBDA database, operated at the Institute for Astronomy of the University of Vienna.

REFERENCES

Avedisova V.S., 2005, ARep, 49, 435
Barniske A., Oskinova L.M., Hamann W.-R., 2008, A&A, 486, 971
Benjamin R.A. et al., 2003, PASP, 115, 953
Blaauw A., 1961, Bull. Astron. Inst. Netherlands, 15, 265
Blum R.D., Damineli A., Conti P.S., 1999, AJ, 117, 1392
Bohlin R.C., 1996, AJ, 111, 1743
Brighenti F., D'Ercole A., 1994, MNRAS, 270, 65
Carey S.J. et al., 2009, PASP, 121, 76
Chevalier R.A., Imamura J.N., 1983, ApJ, 270, 554
de Wit W.J., Testi L., Palla F., Zinnecker H., 2005, A&A, 437, 247
Dehnen W., Binney J.J., 1998, MNRAS, 298, 387
Esteban C., Smith L.J., Vilchez J.M., Clegg R.E.S., 1993, A&A, 272, 299
Fazio G.G. et al., 2004, ApJS, 154, 10
Gies D.R., Bolton C.T., 1986, ApJS, 61, 419
Gvaramadze V.V., 2009, MNRAS, 395, L85
Gvaramadze V.V., Bomans D.J., 2008, A&A, 490, 1071
Gvaramadze V.V., Gualandris A., Portegies Zwart S., 2008, MNRAS, 385, 929
Gvaramadze V.V., Gualandris A., Portegies Zwart S., 2009, MNRAS, 396, 570
Gvaramadze V.V., Kniazev A.Y., Fabrika S., 2009, preprint (astro-ph/0909.0458)
Gvaramadze V.V., et al., 2009, MNRAS, 400, 524
Hamann W.-R., Gräfener G., 2004, A&A, 427, 697
Hamann W.-R., Koesterke L., 1998, A&A, 335, 1003
Hamann W.-R., Feldmeier A., Oskinova L.M., 2008, Clumping in Hot-Star Winds. URN: http://nbn-resolving.de/urn:nbn:de:kobv:517-opus-13981
Hamann W.-R., Gräfener G., Liermann A., 2006, A&A, 457, 1015

Hamann W.-R., Duennebeil G., Koesterke L., Wessolowski U., Schmutz W., 1991,A&A, 249, 443
Helfand D.J., Becker R.H., White R.L., Fallon A., Tuttle S., 2006, AJ, 131, 2525
Hora J.L., et al., 2009, BAAS, 41, 498
Hutsemekers D., 1997, in Nota A., Lamers H.J.G.L.M., eds, ASP Conf. Ser. Vol. 120, Luminous Blue Variables: Massive Stars in Transition. Astron. Soc. Pac., San Francisco, p. 316
Kharchenko N.V., 2001, Kinematika i Fizika Nebesnykh Tel, 17, 409
Kniazev A.Y., Pustilnik S.A., Grebel E.K., Lee H., Pramskij A.G., 2004, ApJS, 153, 429
Kniazev A.Y. et al., 2008a, MNRAS, 388, 1667
Kniazev A.Y. et al., 2008b, MNRAS, 384, 1045
Marston A.P., Welzmiller J., Bransford M.A., Black J.H., Bergman P., 1999, ApJ, 518, 769
Martins F., Plez B., 2006, A&A, 457, 637
Mathis J.S., Cassinelli J.P., van der Hucht K.A., Prusti T., Wesselius P.R., Williams P.M., 1992, ApJ, 384, 197
Meynet G., Maeder A., 2003, A&A, 404, 975
Moffat A.F.J., Drissen L., Robert C., 1989, in Davidson K., Moffat A.F.J., Lamers H.J.G.L.M., eds, Proc. IAU Colloq. 113, Physics of Luminous Blue Variables. Kluwer Academic Publishers, Dordrecht, p. 229
Moneti A., Stolovy S., Blommaert J.A.D.L., Figer D.F., Najarro F., 2001, A&A, 366, 106
Morgan D.H., Parker Q.A., Cohen M., 2003, MNRAS, 346, 719
Oke J.B., 1990, AJ, 99, 1621
Parker Q.A. et al., 2005, MNRAS, 362, 689
Poveda A., Ruiz J., Allen C., 1967, Bol. Obs. Tonantzintla Tacubaya, 4, 86
Price S.D., Egan M.P., Carey S.J., Mizuno D.R., Kuchar T.A., 2001, AJ, 121, 2819
Reid M.J., 1993, ARA&A, 31, 345
Rieke G.H., Lebofsky M.J., 1985, ApJ, 288, 618
Rieke G.H. et al., 2004, ApJS, 154, 25
Robberto M., Ferrari A., Nota A., Paresce F., 1993, A&A, 269, 330
Russeil D., 2003, A&A, 397, 133
Schilbach E., Röser S., 2008, A&A, 489, 105
Seaton M.J., 1979, MNRAS, 187, 73
Shergin V.S., Kniazev A.Y., Lipovetsky V.A., 1996, AN, 2, 95
Skrutskie M.F. et al., 2006, AJ, 131, 1163
Smith L.F., Biermann P., Mezger P.G., 1978, A&A, 66, 65
Smith L.F., Shara M.M., Moffat A.F.J., 1996, MNRAS, 281, 163
Stone R.C., 1991, AJ, 102, 333
van der Hucht K.A., 2001, New Astr. Rev., 45, 135
van der Hucht K.A., 2006, A&A, 458, 453
Wilson T.L., Mezger P.G., Gardner F.F., Milne D.K., 1970, A&A, 6, 364
Zasov A., Kniazev A., Pustilnik S., Pramsky A., Burenkov A., Martin J.-M., 2000, A&AS, 144, 429
Zinnecker H., Yorke H.W., 2007, ARA&A, 45, 481